

# Image Quality Assessment by Dual Tree Complex Wavelet Transform In Fractal Analysis

P.Sabareeswari<sup>1</sup>, Dr.T.Menakadevi<sup>2</sup>

<sup>1</sup>PG Scholar, Department of ECE, Adhiyamaan College Engineering, Hosur, Tamilnadu.

<sup>2</sup>Professor, Department of ECE, Adhiyamaan college of Engineering, Hosur, Tamilnadu.

**Abstract**— *Reduced-reference image quality assessment (RRIQA) provides a practical solution for automatic image quality evaluations in various applications where only partial information about the original reference image is accessible. In this paper, multifractal analysis is personalized to reduced-reference image quality assessment (RR-IQA). A new RR-QA approach is proposed, which measures the difference of spatial arrangement between the reference image and the distorted image in terms of spatial regularity measured by fractal dimension. An image is first shown in wavelet domain using dual tree complex wavelet transform. Then, fractal dimensions are computed on each wavelet sub-band and concatenated as a feature vector. Finally, the extracted features are pooled as the quality score of the distorted image using  $\ell_1$  distance. Compared with existing methods, the proposed approach measures image quality from the perspective of the spatial distribution of image patterns. The proposed method was evaluated on seven public benchmark data sets. Experimental results have demonstrated the excellent performance of the proposed method in comparison with state-of-the-art approaches.*

**Keywords**— *RR-IQA, multifractal, spatial arrangement, wavelet, sub-band, DTCWT*

## I. INTRODUCTION

Reduced-reference (RR) image quality metrics provide a solution that lies between FR and NR models. They are designed to predict the perceptual quality of distorted images with only partial information about the reference images. Recently, the video quality experts group has included RR image/video quality assessment as one of its directions for future development. RR methods are useful in a number of applications. For example, in real-time visual communication systems, they can be used to track image quality degradations and control the streaming resources. The system includes a feature extraction process at the sender side and a feature extraction/quality analysis process at the receiver side. The extracted RR features usually have a much lower data rate than the image data and are typically transmitted to the receiver through an ancillary channel. Although it is often assumed that the ancillary channel is error-free, this is not an absolutely necessary requirement since even partly decoded RR features may still be helpful in evaluating the quality of the distorted image, though the accuracy may be severely affected.

A successful RR quality assessment method must achieve a good balance between the data rate of RR features and the accuracy of image quality prediction. On the one hand, with a high data rate, one can include a large amount of information about the reference image, leading to more accurate estimation of distorted image quality but it becomes a heavy burden to transmit the RR features to the receiver. On the other hand, a lower data rate makes it easier to transmit the RR information, but harder for accurate quality estimation.

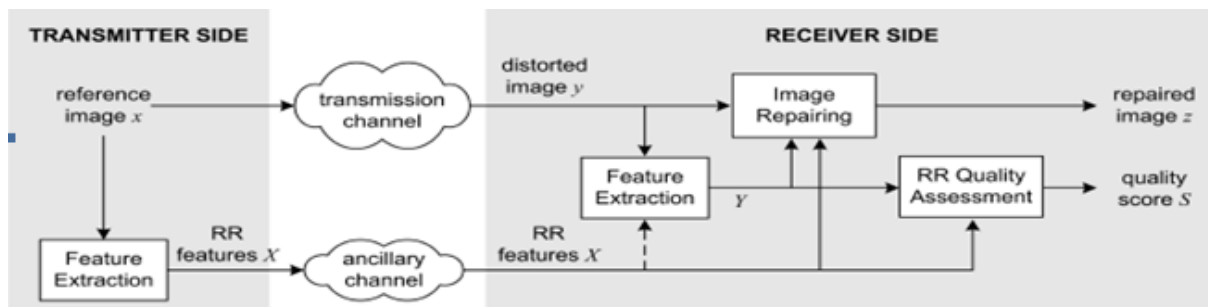


FIG 1. GENERAL FORM OF RR-IQA

The basic assumption behind natural image statistics-based approaches is that most real-world image distortions disturb image statistics and make the distorted image “unnatural”. The unnaturalness measured based on models of natural image statistics can then be used to quantify image quality degradation. In particular, here we observe that the marginal distribution of the wavelet coefficients within a given sub-band changes in different ways for different types of image distortions. We then use an information distance measure between probability distributions to quantify such changes and examine if this provides a useful quality measurement of images through comparisons with subjective image quality evaluations. Since no specific distortion model is assumed, the proposed method is potentially useful for a wide range of distortion types.

Complex wavelets have not been used widely in image processing due to the difficulty in designing complex filters which satisfy a perfect reconstruction property. To overcome this, Kingsbury proposed a dual-tree implementation of the CWT (DT CWT) , which uses two trees of real filters to generate the real and imaginary parts of the wavelet coefficients separately. The two trees are shown in Fig. 3 for 1D signal. Even though the outputs of each tree are down sampled by summing the outputs of the two trees during reconstruction, the aliased components of the signal can be suppressed and approximate shift invariance can be achieved. In this paper CDWT, which is an alternative to the basic DWT the outputs of each tree are down sampled by summing the outputs of the two trees during reconstruction and the aliased. Components of the signal are suppressed and approximate shift invariance is achieved. The DWT suffers from the following two problems.

- Lack of shift invariance - this result from the down sampling operation at each level. When the input signal is shifted slightly, the amplitude of the wavelet coefficients varies so much.
- Lack of directional selectivity - as the DWT filters are real and separable the DWT cannot distinguish between the opposing diagonal directions.

These problems hinder the use of wavelets in other areas of image processing. The first problem can be avoided if the filter outputs from each level are not down sampled but this increases the computational costs significantly and the resulting undecimated wavelet transform still cannot distinguish between opposing diagonals since the transform is still separable. To distinguish opposing diagonals with separable filters the filter frequency responses are required to be asymmetric for positive and negative frequencies. A good way to achieve this is to use complex wavelet filters which can be made to suppress negative frequency components. The CDWT has improved shift-invariance and directional selectivity than the separable DWT.

## II. PRELIMINARIES

Before presenting the detailed description of our approach, we first give an introduction to the two mathematical tools upon which our approach is built.

### 2.1 Dual Tree Complex Wavelet Transform :

The transform is 2-times expansive because The dual-tree complex DWT of a signal  $x$  is implemented using two critically-sampled DWTs in parallel on the same data, as shown in the figure.

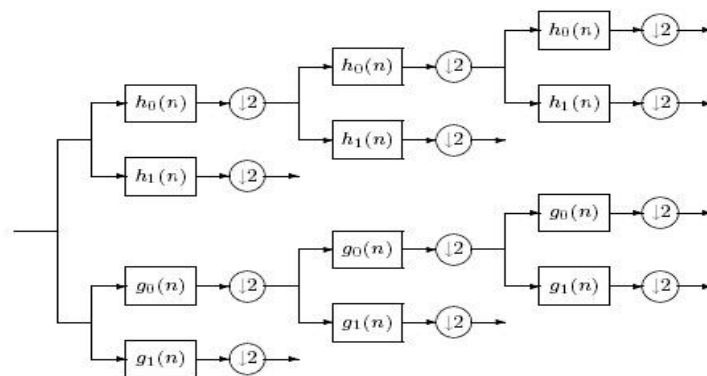


FIG 2.DUAL TREE METHOD

for an N-point signal it gives 2N DWT coefficients. If the filters in the upper and lower DWTs are the same, then no advantage is gained. However, if the filters are designed in a specific way, then the sub-band signals of the upper DWT can be interpreted as the real part of a complex wavelet transform, and sub-band signals of the lower DWT can be interpreted as the imaginary part. Equivalently, for specially designed sets of filters, the wavelet associated with the upper DWT can be an approximate Hilbert transform of the wavelet associated with the lower DWT. When designed in this way, the dual-tree complex DWT is nearly shift-invariant, in contrast with the critically-sampled DWT.

Moreover, the dual-tree complex DWT can be used to implement 2D wavelet transforms where each wavelet is oriented, which is especially useful for image processing. (For the separable 2D DWT, recall that one of the three wavelets does not have a dominant orientation.) The dual-tree complex DWT outperforms the critically-sampled DWT for applications like image denoising and enhancement.

## 2.2 Log Gabor Representation:

The Log-Gabor filters defined in frequency domain are as follows

$$H(\rho, \theta) = \exp\left(-\frac{(\log(\rho/\rho_0))^2}{2(\log(\sigma_\rho/\rho_0))^2}\right) \cdot \exp\left(-\frac{(\theta - \theta_0)^2}{2\sigma_\theta^2}\right),$$

where  $(\rho, \theta)$  are the polar coordinates in frequency domain,  $(\rho_0, \theta_0)$  and  $(\sigma_\rho, \sigma_\theta)$  denote the shift and the bandwidth respectively in the polar coordinates of frequency domain. The term  $\sigma_\rho/\rho_0$  should be held constant to obtain filters with constant shape ratios and its value determines the filter bandwidth. In our implementation, the parameters for generating the Log-Gabor filters are set as:  $\rho_0 = 1/5$ ,  $\theta_0 = 0$ ,  $\sigma_\rho/\rho_0 = 0.75$ , and  $\sigma_\theta = 0.6$ . An example of a 2D Log-Gabor filter in the frequency domain.

## 2.3 Fractal Analysis

Fractal analysis first developed by Mandelbrot provides a powerful mathematical framework to study the irregular, complex and self-similar objects in nature. Fractals can be viewed as the objects with statistical self-similarities. Most of the intensity surfaces of natural images can be modeled by isotropic fractals. One fundamental concept in fractal analysis is the so-called fractal dimension, denoted by  $d$ , which summarizes the irregularity and statistical self-similarity of a given point set  $E$  in some measurement space  $m(\cdot)$  by measuring its power-law behavior according to the scale  $\delta$ :

$$m\delta(E) \propto \delta^{-d}$$

Where  $m\delta(E)$  is some measurement of the given point set  $E$  at scale  $\delta$ . For images, the measurement could be intensity, gradients, or other local image features. There are many techniques to estimate the fractal dimension of image surface.

An efficient approach is the differential box counting (DBC) method, which has advantages in terms of efficiency, accuracy and generality [31]. The DBC method considers an image  $I(x, y)$  of size  $M \times M$  as a 3D point set  $\{(x, y, z) | z = I(x, y)\}$ , where  $(x, y)$  denotes the 2D position and  $z$  denotes the gray level of the image. Suppose the image is scaled down to a size  $s \times s$ , where  $s$  is an integer bounded by  $1 < s \leq M/2$ . Let  $r = s/M$ . The  $(x, y)$  space is partitioned into grids of size  $s \times s$ . A column of boxes of size  $s \times s \times h$  are placed on each grid respectively, where  $h$  denotes the height of a single box.

## III. PROPOSED METHOD

A general framework for the use of RR-IQA in visual communications. An image  $x$  is transmitted to the receiver via a transmission channel, which introduces distortions in the received image  $y$ . Meanwhile, RR features  $X$  extracted at the transmitter side are sent to the receiver through an ancillary channel. The feature extraction unit at the receiver side calculates the features  $Y$  from the received image  $y$  in a similar fashion as in the transmitter side.  $X$  and  $Y$  are compared at the quality assessment unit, which creates a quality score  $S$  of the distorted image  $y$ . A good RR-IQA approach should achieve a good trade-off between rate and accuracy. In general, the larger the rate of the RR features, the more accurate the RR-IQA measure.

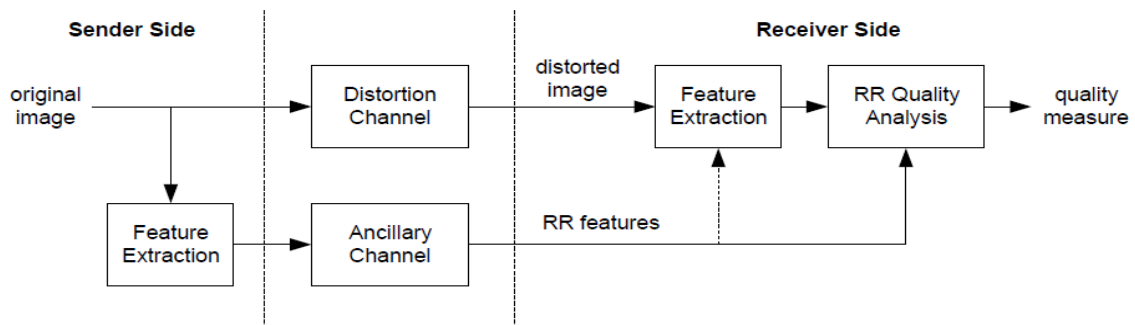


**FIG 3. BLOCK DIAGRAM OF THE PROPOSED METHOD**

Our proposed method is to extract the feature of the image using the dual tree complex wavelet transform (DTCWT). The **Dual-tree complex wavelet transform (DTCWT)** calculates the complex transform of a signal using two separate DWT decompositions (tree *a* and tree *b*). It also provides approximate shift-invariance (unlike the DWT) yet still allows perfect reconstruction of the signal. The design of the filters is particularly important for the transform to occur correctly and the necessary characteristics are:

- The low-pass filters in the two trees must differ by half a sample period
- Reconstruction filters are the reverse of analysis
- All filters from the same orthonormal set
- Tree *a* filters are the reverse of tree *b* filters
- Both trees have the same frequency response

**3.1 Block diagram**

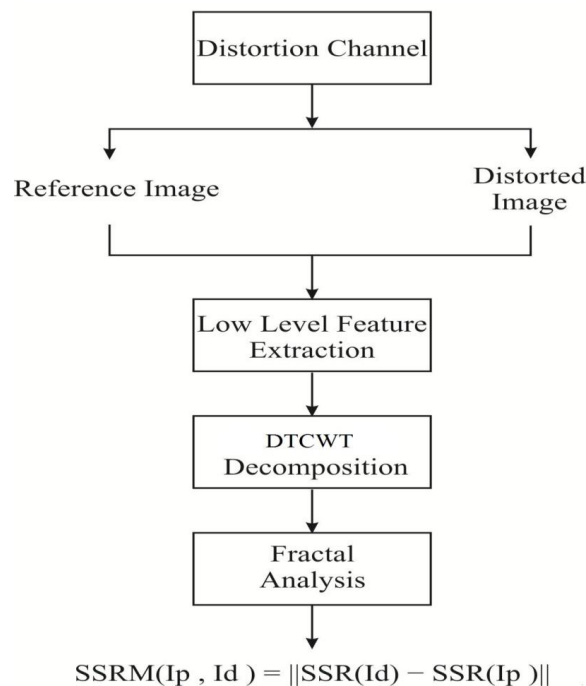


**FIG 4. FLOW CHART**

### 3.2 2D DT-CWT

The 2D DT-CWT also more selectively discriminates features of various orientations. Whereas the critically decimated 2D DWT outputs three orientation selective sub-bands per level conveying image features oriented at the angles of  $90^\circ$ ,  $\pm 45^\circ$ , and  $0^\circ$ , the 2D DT-CWT produces six directional sub bands per level to reveal the details of an image in  $\pm 15^\circ$ ,  $\pm 45^\circ$  and  $\pm 75^\circ$  directions with 4:1 redundancy.

The implementation of 2-D DTCWT consists of two steps. *Firstly*, an input image is decomposed up to a desired level by two separable 2D DWT branches, branch *a* and branch *b*, whose filters are specifically designed to meet the Hilbert pair requirement. Then six high-pass sub bands are generated at each level. HL<sub>a</sub>, LH<sub>a</sub>, HH<sub>a</sub>, HL<sub>b</sub>, LH<sub>b</sub> and HH<sub>b</sub>. *Secondly*, every two corresponding sub bands which have the same pass-bands are linearly combined by either averaging or differencing. As a result, sub bands of 2D DT-CWT at each level are obtained as

$$(LH_a+LH_b)/\sqrt{2},(LH_a-LH_b)/\sqrt{2},(HL_a+HL_b)/\sqrt{2},$$

$$(HL_a-HL_b)/\sqrt{2},(HH_a+HH_b)/\sqrt{2},(HH_a-HH_b)/\sqrt{2},$$

The six wavelets defined by oriented shown above have the sum/difference operation is orthonormal, which constitutes a perfect reconstruction wavelet transform. The imaginary part of 2D DT-CWT has similar basis function as the real part [8]. The 2D DT-CWT structure has an extension of conjugate filtering in 2D case. The filter bank structure of 2D dual-tree is shown in figure

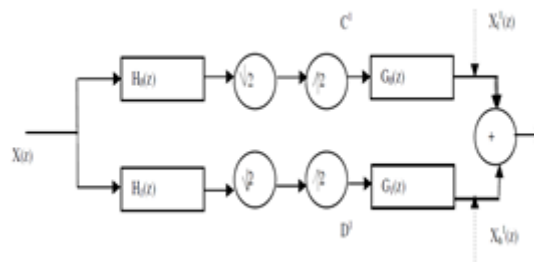


FIG 5.DWT FILTER BANK

Similarity Index of Spatial Regularity:

$$SSR(I)=\omega_{DBC}(G\rho, \theta(m(P_i(I))))$$

$$SSRM(I_p, I_d)=\|SSR(I_p)-SSR(I_d)\|$$

#### IV. EXPERIMENTAL RESULTS

In order to simulate the perception of human to image via the V1 cortex of primates, the Log-Gabor filters  $\{H(\rho, \theta)\}_{\rho, \theta}$  are run on the feature image *M* to localize the image structures of different orientations and frequencies. This procedure results in multiple response images  $\{G\rho, \theta\}_{\rho, \theta}$  from the feature

image:

$$G\rho, \theta(M)=F(M, H(\rho, \theta)),$$

Where  $F(\cdot, H)$  denotes filtering with the Log-Gabor filter *H*. By using Log-Gabor filtering, we convert the extracted image features from image space into visual perceptive space. Then, parallel to characterizing the spatial distribution of the visual responses in the V1 area of HVS, we extract features from the Log-Gabor response images via fractal analysis.

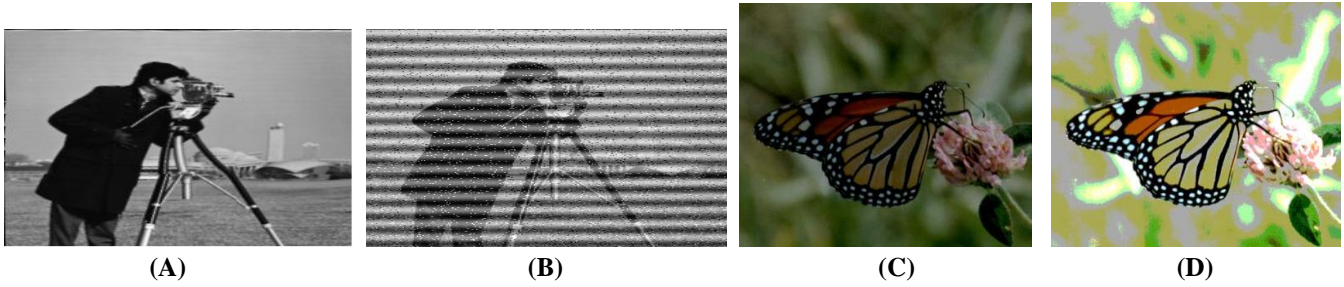


**FIG 6. THE DISTORTED IMAGE BEFORE DECOMPOSITION A) DISTORTION, B) RESTORED IMAGE, C) . IMAGE WITH POOR CONTRAST, D) IMAGE ENHANCEMENT BY CONTRAST STRETCHING**

Comparison between reference image and distorted image using DTCWT is shown below

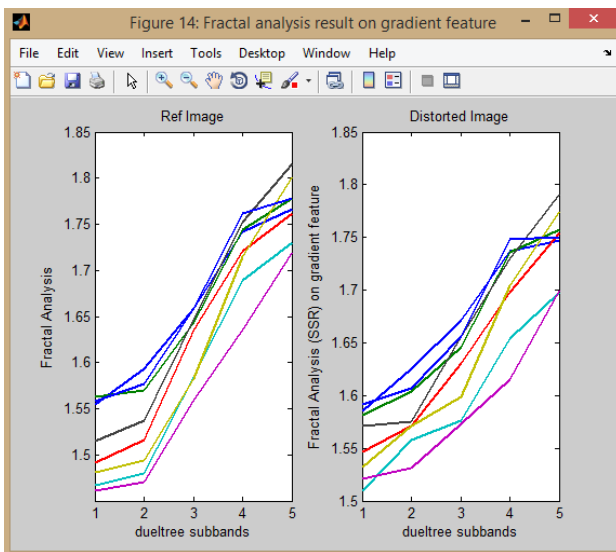


**FIG 7.FRACTAL ANALYSIS RESULT ON GRADIENT FEATURE**

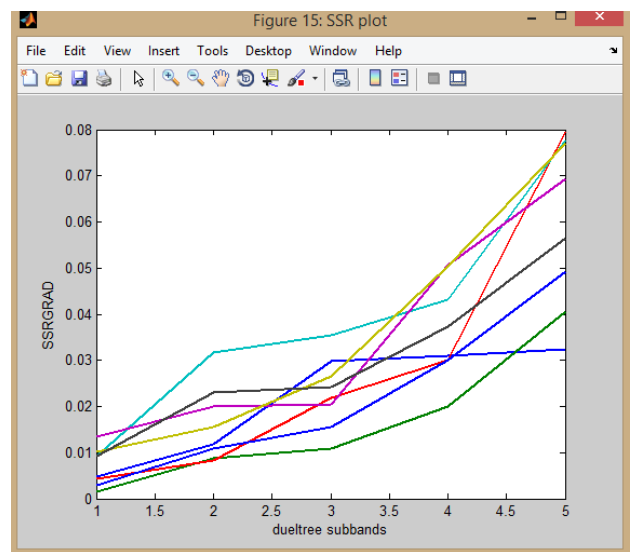


**FIG 8. SSR PLOT**

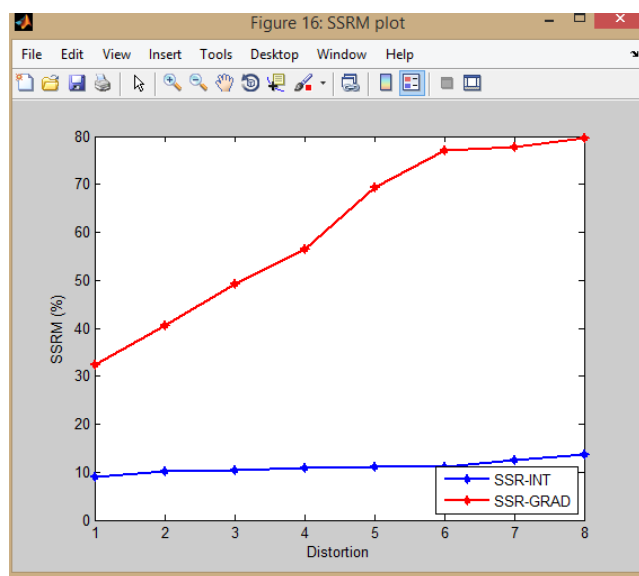


**FIG 9. SSRM PLOT**

By the fractal analysis, it is give as in SSRM curves with the respective distortions .

**TABLE 1**  
**COMPARISON BETWEEN LOG GABOR AND DTCWT**

s.no	image	noise	Log gabor(%)	Dual tree(%)
1	Image1	Salt and pepper	60	68
2	Image2	Gaussian	72	77
3	Image3	Speckle	74	81
4	Image4	Poisson	64	68

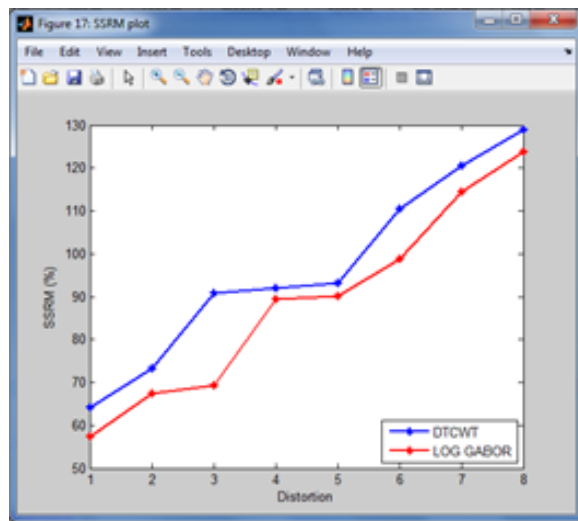


**FIG 10. COMPARISON OUTPUT BETWEEN LOG GABOR AND DTCWT**

## V. CONCLUSION AND FUTURE ENHANCEMENT

In this paper, the design of RR objective perceptual image quality metrics for wireless imaging has been presented. Instead of focusing only on artifacts due to source encoding, the design follows an end-to-end quality approach that accounts for the complex nature of artifacts that may be induced by a wireless communication system. Image quality assessment can assist several image-related tasks including image processing and image recognition. However, image quality assessment is a challenging task, especially when only part information of the reference image is known. We extracted the low level feature and use dual tree complex wavelet transform for decomposition of the image. This extracts the spatial frequency components of the image. For characterizing the distortion we use RRIQA is used. Fractal analysis is employed to characterize the spatial distributions of image structured expressed in Log-Gabor sub-bands of both the reference image and the distorted image. The results show that our method is competitive against the state-of-the-art approaches.

In future the spectrum of spatial regularity can be obtained by various decomposition methods are used and their performance is analyzed.

## REFERENCES

- [1] Yong Xu, Delei Liu, YuhuiQuan, and Patrick Le Callet , Fractal Analysis for Reduced Reference Image Quality Assessment IEEE TRANSACTIONS ON IMAGE PROCESSING, VOL. 24, NO. 7, JULY 2015
- [2] A. Rehman and Z. Wang, "Reduced-reference image quality assessment by structural similarity estimation," IEEE Trans. Image Process., vol. 21, no. 8, pp. 3378–3389, Aug. 2012.
- [3] H. R. Sheikh and A. C. Bovik, "Image information and visual quality," IEEE Trans. Image Process., vol. 15, no. 2, pp. 430–444, Feb. 2006.

- 
- [4] N. Damera-Venkata, T. D. Kite, W. S. Geisler, B. L. Evans, and A. C. Bovik, "Image quality assessment based on a degradation model," *IEEE Trans. Image Process.*, vol. 9, no. 4, pp. 636–650, Apr. 2000.
- [5] L. Zhang, L. Zhang, X. Mou, and D. Zhang, "FSIM: A feature similarity index for image quality assessment," *IEEE Trans. Image Process.*, vol. 20, no. 8, pp. 2378–2386, Aug. 2011.
- [6] H. R. Sheikh, A. C. Bovik, and L. Cormack, "No-reference quality assessment using natural scene statistics: JPEG2000," *IEEE Trans. Image Process.*, vol. 14, no. 11, pp. 1918–1927, Nov. 2005.
- [7] Z. Wang, A. C. Bovik, and B. L. Evans, "Blind measurement of blocking artifacts in images," in *Proc. IEEE Int. Conf. Image Process.*, vol. 3, Sep. 2000, pp. 981–984.
- [8] Z. Wang, H. R. Sheikh, and A. C. Bovik, "No-reference perceptual quality assessment of JPEG compressed images," in *Proc. IEEE Int. Conf. Image Process.*, vol. 1, Sep. 2002, pp. I-477–I-480.
- [9] X. Gao, W. Lu, D. Tao, and X. Li, "Image quality assessment based on multiscale geometric analysis," *IEEE Trans. Image Process.*, vol. 18, no. 7, pp. 1409–1423, Jul. 2009.
- [10] U. Engelke, M. Kusuma, H. J. Zepernick, and M. Caldera, "Reduced-reference metric design for objective perceptual quality assessment in wireless imaging," *Signal Process., Image Commun.*, vol. 24, no. 7, pp. 525–547, 2009.
- [11] Q. Li and Z. Wang, "Reduced-reference image quality assessment using divisive normalization-based image representation," *IEEE J. Sel. Topics Signal Process.*, vol. 3, no. 2, pp. 202–211, Apr. 2009.
- [12] R. Soundararajan and A. C. Bovik, "RRED indices: Reduced reference entropic differencing for image quality assessment," *IEEE Trans. Image Process.*, vol. 21, no. 2, pp. 517–526, Feb. 2012.
- [13] Z. Wang and E. P. Simoncelli, "Reduced-reference image quality assessment using a wavelet-domain natural image statistic model," *Proc. SPIE*, vol. 5666, pp. 149–159, Mar. 2005.
- [14] W. Xue and X. Mou, "Reduced reference image quality assessment based on Weibull statistics," in *Proc. 2nd Int. Workshop Quality Multimedia Exper.*, 2010, pp. 1–6.
- [15] L. Ma, S. Li, F. Zhang, and K. N. Ngan, "Reduced-reference image quality assessment using reorganized DCT-based image representation," *IEEE Trans. Multimedia*, vol. 13, no. 4, pp. 824–829, Aug. 2011.